Raman spectra of thermally excited Brazil nut oil and experimental and theoretical correlation of oleic acid

Q. S. Martins[a], A. F. Sonsin[a], L. G. F. Silva[b], A. Ribas[a], D. L. L. Oliveira[a], and R. C. S Lima[a]

[a]*Fundação Universidade Federal de Rondônia - UNIR, RO, Brazil.*
e-mail: quesle.martins@unir.br
[b]*Instituto Federal de Educação, Ciência e Tecnologia - IFRO, RO, Brazil.*

Received 13 February 2024; accepted 4 August 2024

In this study, Raman spectra of Brazil nut oil were collected through a frying process at temperatures ranging from 50°C to 250°C, and of oleic acid at room temperature to compare their respective vibrational bands.The theoretical and scaled Raman frequencies of oleic acid structure were obtained with Density Functional Theory (DFT), using the ccpVDZ, 631G, 6-311G+(d,p) basis set and B3LYP and CAMB3LYP functionals. Experimental results reveal subtle changes in the spectra of Brazil nut oil from 210°C onwards, characterized mainly by a decrease in the Raman signal and broadening of certain bands, such as those observed at 1746 cm^{-1}, 2726 cm^{-1} and 3012 cm^{-1}. At temperatures around 230°C to 250°C Brazil nut oil undergoes advanced thermal degradation. The linear fit data demonstrate a linear relationship between the Raman signal and temperature increase, with R^2 values of 0.999 and 0.977, for some bands. The DFT method proved to be useful in predicting oleic acid spectra and vibrational signatures were assigned with the help of the VEDA program. This work highlights the potential of Raman spectroscopy to detect changes in Brazil nut oil during frying.

Keywords: Raman spectroscopy; density functional theory; Brazil nuts oil; thermal analysis.

DOI: https://doi.org/10.31349/RevMexFis.71.010502

1. Introduction

Bertholletia excelsa, also known as the Brazil nut tree or Brazil nut, is a native species of the Amazon rainforest and is highly regarded for its potential in agroforestry systems. The Brazil nut itself is edible, and the oil extracted from its seeds through cold pressing, known as Brazil nut oil (BNO), is abundant in fatty compounds [1–3]. The consumption of Brazil nut oil has been linked to anti-aging effects and immune system stimulation, making it socially and economically significant [4–6]. As a vegetable oil, BNO possesses a high concentration of triglycerides. It is rich in fatty acids (FA) [7], which can be classified into two main types: saturated fatty acids (SFA) and unsaturated fatty acids (UFA). SFA consists of long carbon chains with only single carbon-carbon (C-C) bonds, while UFA contains double carbon-carbon (C=C) bonds and can be further divided into monounsaturated fatty acids (MUFA) and polyunsaturated fatty acids (PUFA). Saturated fats are unreactive, whereas unsaturated fats can undergo various types of reactions [8, 9]. Due to their extensive applications in the food, pharmaceutical, and industrial sectors, vegetable oils such as BNO have garnered significant interest across various fields [10, 11]. However, during cooking processes, vegetable oils can potentially pose health risks, particularly when contaminated with impurities [12, 13] or when reused, leading to problems associated with thermal degradation (oxidation). BNO contains a higher concentration of the monounsaturated fatty acid oleic acid (OA) [1,3,14]. In this study, we collected Raman spectra of BNO samples that underwent stimulated thermal degradation. We also collected Raman spectra of pure OA to compare them with the natural bands found in BNO. Raman spectroscopy has been extensively employed to distinguish and monitor different types of edible oils, including analyzing their smoke point [8, 9, 15, 16]. To collect the Raman spectra, a 5 mL sample of BNO was divided into eight equal portions (samples A, B, C, D, E, F, G e H). Each portion was subjected to different temperatures ranging from 50°C to 250°CȦ Raman spectrum of pure OA, without any thermal treatment, was also obtained. Density Functional Theory (DFT) calculations were performed on the oleic acid structure to obtain theoretical frequencies. The VEDA program was used to assign theoretical vibrational signatures [17, 18, 20]. The results obtained from the Raman spectra can provide a quick assessment of the conditions of stimulated thermal degradation of BNO, while the identification of OA bands can offer insights into structural changes within the sample. The utilization of the DFT method is expected to aid in identifying the vibrational modes of both BNO and OA, as well as in understanding the spectral arrangement of fatty acids. This study is groundbreaking in its acquisition of Raman spectra that depict the thermal behavior of BNO and the comparison of vibrational bands with both experimental and theoretical OA data. The primary objective of this research is to expand the application of experimental and theoretical Raman spectroscopy as a valuable tool for the rapid and reliable analysis of edible vegetable oils and the detection of fatty acids within their composition.

2. Materials and methods

2.1. Material and experimental

Raman spectra of BNO and 99% oleic acid (OA99) samples were obtained using a Horiba Xplora Series Raman spectrometer, equipped with a single 532 nm laser and a spectral range of 560 to 3500 cm^{-1}. The spectrometer was located at the Federal University of Alagoas (UFAL). The BNO samples, divided into eight equal parts, were provided by Inovam Brasil, based in Ji-Paraná - RO. A 5 mL sample of BNO was divided into eight equal portions (A, B, C, D, E, F, G and H). Each portion was subjected to heating measurements in an EDG 1800 muffle furnace once. At 50°C (sample A), 100°C (B), 150°C (C), 170°C (D), 190°C (E), 210°C (F) and G and H at 230 and 250°C, respectively. Once the temperature was reached in the muffle, it was left to act for 20 minutes so that all the material reached temperature.

Raman spectra were collected 15 minutes after removing the samples from the muffle furnace, at room temperature. The OA99 sample was provided by the Nanomaterials and Nano Biomagnetism Laboratory at the Federal University of Rondônia (UNIR) and the Raman spectrum was collected at room temperature. The spectra were smoothed using Savitzky-Golay, with second-order polynomials and baseline in the Origin program.

2.2. Computational

Theoretical frequencies were obtained by calculating the structure of oleic acid ($C_{18}H_{34}O_2$) using the Density Functional Theory (DFT) method in the GAUSSIAN 09 software [21]. The DFT approximation provides an overview of vibrational behavior. The CAMB3LYP (CB3LYP) and B3LYP functionals and the base set 631G, ccpVDZ and the polarized base 6-311G+(d,p) were used. CB3LYP and B3LYP are three-parameter hybrid Becke functionals, *i.e.*, they are series of hybrid functionals, which include a mixture of Hartree-Fock exchange with DFT exchange correlation [22]. CB3LYP is' long-range corrected version of B3LYP using the Coulomb attenuation method [23]. The ccpVDZ, 631G, 6311G+(d,p) basis sets are recommended for the optimization of organic molecular groups. The presence of diffusion (+) and polarization functions ("d" and "p") tend to increase the precision of calculations for hydrogen and oxygen atoms, respectively [17, 18]. The cc-pVDZ basis set has had redundant functions removed to increase computational efficiency and includes polarization functions by definition [19]. Vibrational assignments and potential energy distribution (PED) analysis were performed with a high level of precision using the VEDA program [20]. To match the theoretical frequencies with the experimental ones, a scaling factor (SF) of 0.967 was applied for adjustment purposes.

3. Results and discussion

3.1. BNO Raman spectra

Figures 1 and 2 depict the Raman spectra of the BNO samples obtained at various temperatures ranging from 50°C to 250°CFigure 1 shows the spectral region spanning 560-1800 cm^{-1}, while Fig. 2 was focused on the range of 2560 - 3500 cm^{-1}. Figure 1 the bands at 1440 cm^{-1}, 1658 cm^{-1} and 1746 cm^{-1} can be attributed to the symmetric stretching vibrations of CC groups, C=C bonds and C=O groups, respectively [3, 24]. Figure 2 shows peaks at 2726 cm^{-1} (CH), 2855 cm^{-1} (CH2), and 2094 cm^{-1} (CH3) [25, 26]. These peaks correspond to symmetric and asymmetric stretching modes of methylene and methyl groups, which are abundant in edible oils [27]. Furthermore, the band around 3012 cm^{-1} can be assigned to symmetric and asymmetric stretching vibrations of the *cis* HC=CH group, commonly found in unsaturated fatty acids [24]. It is worth noting that these groups exhibit significant shifts in this region when connected to an unsaturated group [28, 29].

Additionally, in Fig. 1 a broad and low-intensity band can be observed at 730 cm^{-1}, which is likely attributed to OH

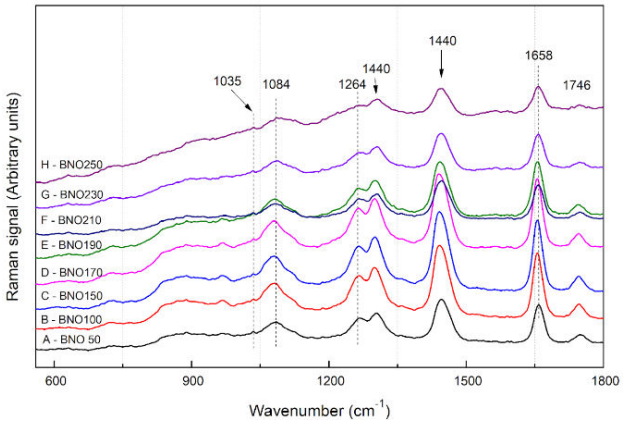

FIGURE 1. Heating measures. Raman spectra of thermal BNO for the region from 560 to 1800 cm^{-1}.

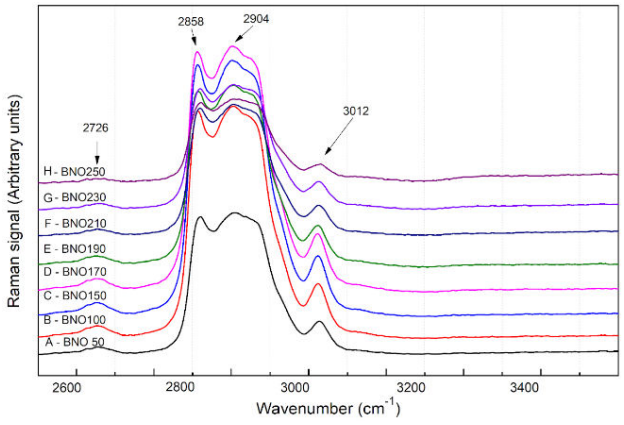

FIGURE 2. Heating measures. Raman spectra of thermal BNO for the region from 2560 to 3500 cm^{-1}.

deformation (or torsion OHCC). The peak at 868 cm^{-1} corresponds to skeletal chain vibrations, while the peaks at 966 cm^{-1} and 1084 cm^{-1} may be associated with *trans* bending vibrations of C=C bonds [16, 25, 30]. It is noteworthy that the peak at 966 cm^{-1} is clearly observed in samples B, C, D, and E, while it is less pronounced in the other spectra (samples A, G, and H). However, this peak is clearly visible in the Raman spectrum of OA shown in Fig. 5, along with peaks at 1086 cm^{-1}, 1265 cm^{-1}, 1302 cm^{-1}, 1438 cm^{-1}, 1658 cm^{-1}, 1742 cm^{-1}, 2722 cm^{-1}, and 3008 cm^{-1}. Changes in the region around 966 cm^{-1} may not be directly related to potential oxidative factors of the sample or the frying process of the oil, but rather a consequence of external factors during heating [16]. The increase in energy during heating can impact common groups present in the sample, such as CH groups, which are susceptible to temperature variations. Additionally, intermolecular and intramolecular interactions of lipids can be affected by the composition of the sample and the surrounding matrix/environment [25, 31]. However, oxidative reactions result in the formation of cyclic monomeric triglycerides, essentially the product of intramolecular rearrangement catalyzed by changes in the aliphatic groups adjacent to C=C bonds, resulting in stereo mutation and unsaturation in the aliphatic chains of the C=C bonds formed in both *cis* and *trans* configurations during the frying process [15, 32]. The absence of the peak in samples F to H, together with the relative decrease in the Raman signal and the slight broadening of certain peaks in the late phase, is evident. Figure 3 provides a detailed analysis of the decrease in the Raman signal as a function of temperature for the most representative bands in Fig. 1 and 2. The data in Fig. 3 reveals that the selected modes show a progressive change in the intensity of the Raman signal with varying temperature, with greater drops observed for values above 150°C.

Figure 4 demonstrates a linear fitting of the data, particularly for the band centered at 2726 cm^{-1}, which displays a higher level of linearity among the observed quantities, with an R^2 value of 0.999. For the 3012 cm^{-1} band, there is a good fit, although it has the lowest measured R^2 value of 0.977. This suggests that functional groups associated with this band are more sensitive to structural factors resulting from temperature variations. However, these changes may be more prominent for values exceeding 190°C. Changes in the Raman signals observed at 1264 cm^{-1}, 1300 cm^{-1}, 1440 cm^{-1}, 1658 cm^{-1}, 1746 cm^{-1}, 2726 cm^{-1}, and 3012 cm^{-1} in Figs. 1 and 2 suggest a process of thermal oxidation aging, particularly for values exceeding 210°C in the samples. Among these peaks, the ones at 1264 cm^{-1} and 3012 cm^{-1} can serve as more sensitive indicators of thermal degradation [1, 16].

Theoretical considerations suggest that carbon-carbon (CC) single bonds are relatively stable during thermal oxidation or heating, with only minimal oxidation occurring [33]. However, changes in density and potential breakage of carbon-carbon double bonds (C=C) can be expected [12]. These factors can shed light on the behavior of oils at their

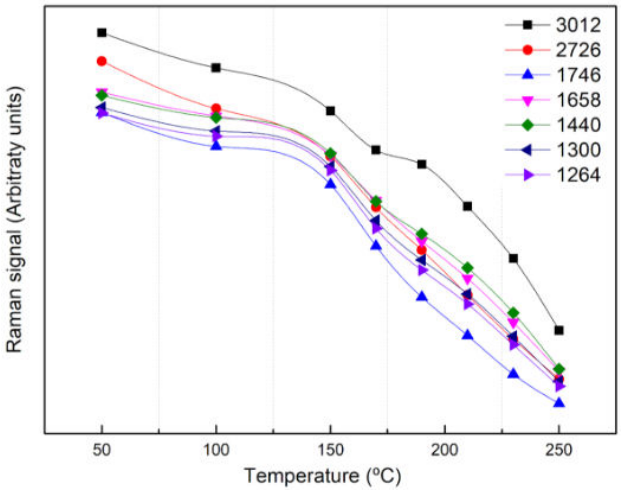

FIGURE 3. Relationship between decrease in Raman signal of BNO bands with temperature variation.

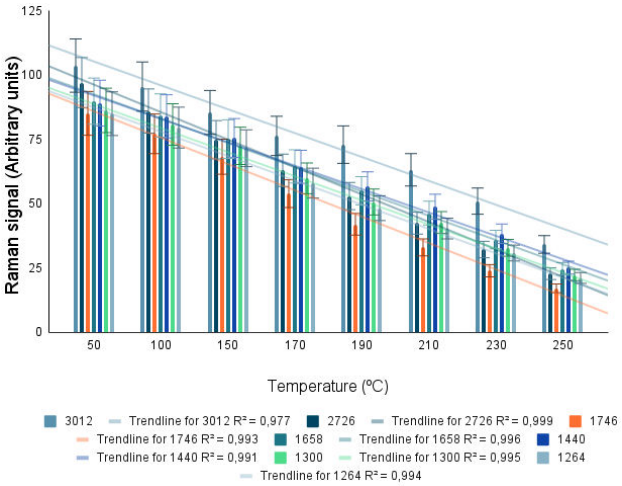

FIGURE 4. Trendlines of Raman signals of BNO bands as a function of temperature.

smoke point. This observation aligns with the findings reported by Bennion and Hanning [34] and Yoon *et al*. [35], who noted that an increase in acid value correlates with a decrease in smoke point. This relationship indicates that the smoke point of oils is associated with the decomposition of the molecular mass, as well as the presence of free fatty acids (FFA) and partial glycerides [36]. Moreover, vegetable oils are rich in triacylglycerols, which are lipids composed of a glycerol molecule esterified with fatty acids. The properties of these oils, such as crystallization and melting point, are greatly influenced by the length of the fatty acid chain and whether it is saturated or unsaturated.

At temperatures exceeding 250°C BNO displays signs of degradation, indicating that the C=C double bonds in BNO undergo accelerated thermal oxidation during heating. This is a common tendency observed in oils containing unsaturated fatty acids (UFA) [16]. When unsaturations are present, the fatty acids become more branched, resulting in decreased

molecular packing and influencing the melting points of unsaturated triacylglycerols, which are lower compared to those containing only saturated fatty acids (SFA) [37]. The peaks at 730 cm^{-1} and 1035 cm^{-1} in Fig. 1 as well as 2858 cm^{-1} and 2904 cm^{-1} in Fig. 2, do not provide significant contributions to the identification of the smoke point of the sample, especially for measurements below 210°C.The primary peaks of BNO do not exhibit significant changes in their position (wavenumber).

3.2. Oleic acid spectrum

The Raman spectrum of OA99, the main component of BNO [1, 3], is shown in Fig. 5. The peaks at at 1086 cm^{-1}, 1265 cm^{-1}, 1302 cm^{-1}, 1438 cm^{-1}, 1658 cm^{-1}, 1742 cm^{-1}, 2722 cm^{-1}, and 3008 cm^{-1} are observed and show similarity to the spectra shown in Figs. 1 and 2. The peaks at 1438 cm^{-1}, 1658 cm^{-1}, and 1742 cm^{-1} correspond to symmetric stretching modes of CH, C=C and C=O bonds, respectively.

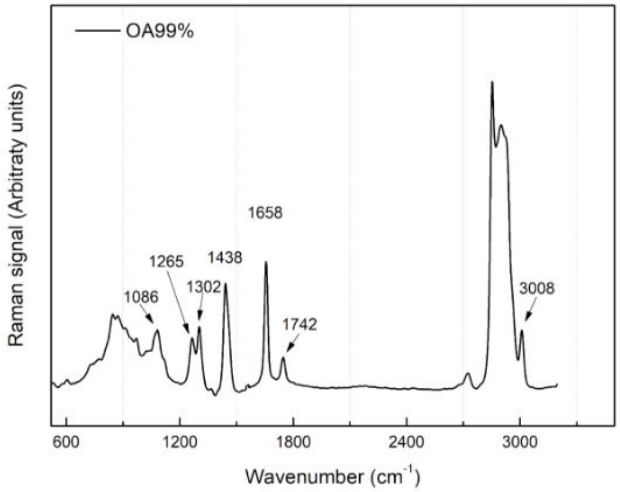

FIGURE 5. Experimental Raman spectrum of oleic acid 99% (OA99).

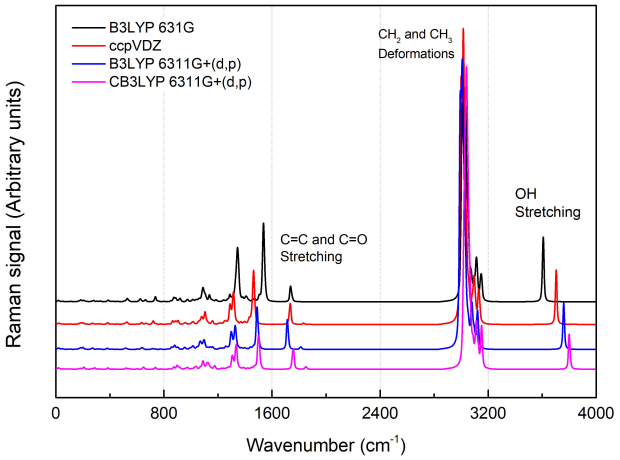

FIGURE 6. Theoretical Raman spectra of oleic acid. B3LYP 631G (B/631G), B3LYP 6311G+(d,p) (B/6311G+(d,p)), CAMB3LYP 6311G+(d,p) (CB/6311G+(d,p)) and ccpVDZ.

Symmetrical and asymmetric stretching are observed at 2850 cm^{-1} (CH_2), 2898 cm^{-1} (CH_3), and *cis* HC=CH bonds are shown at 3008 cm^{-1}.

With the presence of these peaks, the OA99 spectrum effectively explains the identification of Raman peaks in BNO and can be extended to a range of vegetable oils, such as olive oil [38–40], palm oil, and soybean oil [41], canola oil [42], coconut oil [43], and also ostrich oil [44].

3.3. Calculation

The theoretical Raman spectra of oleic acid (OA_{calc}) in the DFT method are shown in Fig. 6. In Fig. 7, the electrostatic potential (MEP) map is shown. Table I provides some experimental wavenumbers of BNO and OA99, and calculated and scaled. This one, with a scale factor (SF) of 0.967 [45, 46]. Still in Table I, the vibrational assignments of the groups are presented, followed by the number of each atom in the molecule, its symbol and percentage of contribution given by the maximum energy parameter, PED [20].

In Fig. 6, the main vibrational peaks observed in the Raman spectrum of oleic acid are located around 636 cm^{-1}, 878 cm^{-1}, 1099 cm^{-1}, 1296 cm^{-1}, 1325 cm^{-1}, 1491 cm^{-1}, 1714 cm^{-1} (C=C), 1812 cm^{-1} (C=O), 2995 cm^{-1}, 3012 cm^{-1}, 3027 cm^{-1}, 3083 cm^{-1} (asymmetric methyl), 3098 cm^{-1} (*cis* asymmetric), 3122 cm^{-1} (HC=CH *cis* symmetric), and 3759 cm^{-1} (OH). The peaks present in Fig. 6 for OA_{calc} indicate the predominance of fatty acid groups corresponding to the BNO sample. In the experimental spectra (Figs. 2 and 5), does not is observed symmetric OH band above 3250 cm^{-1}, but is present in the OA_{calc} spectra in Fig. 6. Furthermore, Fig. 6 shows a shift of peaks for large wavenumbers, this happens exactly for basis sets with polarization and diffusion functions. Therefore, frequencies were adjusted using the scale factor of 0.967, as indicated in Table I. The scaled values are important for assigning the corresponding vibrational signatures and helps compensate for vibrational anharmonicity errors and incomplete treatment of electronic mechanics, as described in the Computational Chemistry Comparison and Benchmark DataBase [46]. Theoretical results (Table I) show that larger base sets [such as CB/6311G+(d,p)]

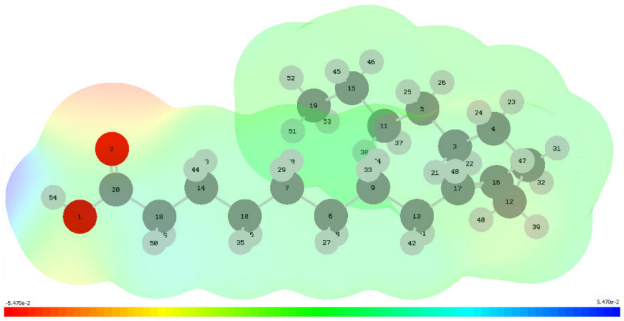

FIGURE 7. Surface electrostatic potential (MEP) map of oleic acid structure from DFT.

TABLE I. Experimental and theoretical scaled frequencies. Used scale factor of 0.967. Next to the theoretical frequencies, the percentage (%) of vibrational contribution in VEDA. Vibration assignments are also presented.

Experimental		Theoretical scaled / (PED%)				
BNO	OA99	B/631G	ccpVDZ	B/6311G+(d,p)	CB/6311G+(d,p)	Assignments
- -	- -	3488 / (100)	3582 / (100)	3635 / (100)	3675 / (100)	υ_s (1 54) (OH)
3012	3008	3017 / (55)	3029 / (57)	3030 / (58)	3047 / (56)	υ_s(17 48) *cis*(=CH)
- -	- -	3044 / (57)	3004 / (55)	2996 / (56)	3024 / (49)	υ_{as}(16 47) *cis*(=CH)
- -	- -	3010 / (72)	2995 / (74)	2981 / (74)	3011 / (41)	υ_{as}(19 52) (CH_3)
- -	- -	2943 / (35)	2930 / (43)	2927 / (39)	2956 / (31)	υ_s(18 50) (CH_2)
2964	2893	3005 / (46)	2988 / (47)	2917 / (37)	3002 / (44)	υ_s(19 51) (CH_3)
2904	2900	2928 / (27)	2917 / (30)	2913 / (27)	2967 / (26)	υ_s(8 32) (CH_2)
2726	2722	- -	- -	- -	- -	*Undefined*
1746	1742	1693 / (81)	1773 / (85)	1752 / (85)	1791 / (85)	υ_s(2 20) (O=C)
1658	1658	1681 / (81)	1677 / (74)	1657 / (72)	1698 / (73)	υ_s(17 16) (C=C)
1440	1438	1423 / (39)	1382 / (30)	1442 / (35)	1402 / (33)	δ_{sci}(48 17 16) (HCC)
1300	1302	1301 / (17)	1262 / (13)	1281 / (14)	1301 / (15)	δ_{ω}(43 14 18) (HCC)
1264	1265	1423 / (38)	1382 / (29)	1253 / (17)	1402 / (31)	δ_t(47 16 17) (HCC)
1084	1086	1067 / (18)	1062 / (26)	1052 / (27)	1071 / (23)	υ_s(4 8) (CC)
1035	1035	1004 / (20)	977 / (21)	1001 / (10)	1004 / (23)	τ(47 16 17 13) (HC=CH)
847	846	837 / (49)	855 / (53)	849 / (52)	868 / (53)	υ_s(20 18) (CC)
730	727	640 / (67)	646 / (62)	706 / (55)	626 / (55)	τ(54 20 1 18) (HOCC)
638	636	606 / (53)	614 / (60)	615 / (60)	626 / (61)	δ_{sci}(2 20 1) (OCC)
606	603	593 / (53)	583 / (17)	584 / (17)	582 / (15)	δ(13 17 16) (CCC)

Legend: Stretching; υ_s = symmetrical; υ_{as} = asymmetrical. Bending; δ_{sci} =scissor; δ_t = twist; δ_{ω} = wagg and τ = torsion.

present disharmony in relation to base sets with fewer functions. Percentage contribution values per molecular group show greater agreement for most of the frequencies indicated.

The computational method generates a displacement of these bands from their expected positions, suggesting that the bands are displaced in that direction. This change may be related to CH groups around 3000 cm^{-1}. The overestimated results obtained through computational calculations are expected, since the process assumes electron density free of any external disturbances. Because Raman spectroscopy relies on detecting vibrations induced by changes in electrical polarizability, polar molecular groups tend to exhibit low or no activation in Raman measurements [15, 49]. Considering the high content of fatty acids in BNO, this studies can contribute to the qualitative analysis of the product under heat stress, helping to investigate the formation of radicals in both saturated and unsaturated fats [12].

The MEP (Fig. 7) shows how the charge density is distributed in the structure. Hydrogen bond present in the oleic acid structure represents an observation factor, since such interactions also determine physical properties, such as the melting point or boiling point of substances [47]. On the MEP a color scale from red to dark blue. These regions show interactions of hydroxyl and carbonyl groups and are electronegatively labeled with respect to the Hirshfeld surface [48]. Table I shows numbers and atoms of different functional groups.

4. Conclusion

This study provided insights into the spectral changes associated with the thermal degradation of BNO. The peaks at 1264, 1440, 1658, 1743, 2726 and 3012 cm^{-1} were identified as important in establishing a strong correlation with the oleic acid peaks (OA99). For temperatures above 210°C they showed changes such as a decrease in Raman signal intensity and a slight broadening of bands, indicating the progression of thermal degradation. The linear regression analysis indicates a certain degree of linearity, with R^2 values of 0.999 and 0.977, respectively.

The results demonstrated that RS could be a relevant technique to evaluate the oxidation state of BNO because the oxidation parameters were quickly determined. The combined with DFT provided an overview of the vibrational behavior. This study contributes to the qualitative and rapid assessment of the behavior of saturated and unsaturated fats under thermal stress. It increases our understanding of the changes that occur in these fats and their potential implications for assessing quality in a non-destructive and direct way.

Acknowledgments

The authors would like to thank the Optics and Nanoscopy Group (GON) at the Universidade Federal de Alagoas (UFAL), the Light Scattering Laboratory at Instituto de Física at Universidade Federal de Mato Grosso (UFMT), as well as the Research in Experimental and Applied Physics and Structure of Matter and Computational Physics groups at Universidade Federal de Rondônia (UNIR) for their support and collaboration. Special thanks are given to the PIBIC-UNIR grant number 2021/Pibic/Dpesq/Propesq/2021 and FAPERO (Grant 009/2022) for financial support.

Author statement

Q.S. Martins: Conceptualization, Methodology, Project administration, Writing - Original Draft. L.G.F Silva, Q.S. Martins: Data curation, Visualization, Investigation, Writing - Original draft preparation. R.C.S Lima, A. Ribas, D.L. Oliveira: Visualization. L.G.F Silva, Q.S. Martins: Software, Validation, Data curation. L.G.F Silva, A. F. Sonsin: Supervision, Project administration, Methodology, Writing Reviewing and Editing.

Declaration of interests: The authors declare no conflict of interest relationship in this paper.

1. M.A.P. Muniz *et al*., Physicochemical characterization, atty acid composition, and thermal analysis of Bertholletia excelsa HBK oil. *Pharmacogn Mag.* **11** (2015) 147, https://doi.org/10.4103/0973-1296.149730.
2. Q.S. Martins, C.A. Aguirre, J. Farias, Approach by Raman and infrared spectroscopy in three vegetable oils from the Brazilian Amazon, *Rev. Mex. Fis.*, **4** (2019) 328, https://doi.org/10.31349/RevMexFis.65.328.
3. Q.S. Martins, L.M.S.Santos, J.L.B.Faria, Raman spectra and ab-initio calculations in Bertholletia excelsa oil, *Vib. Spectrosc.* **106** (2020) 102986, https://doi.org/10.1016/j.vibspec.2019.102986.
4. B. R. Cardoso, G. B. S. Diarte, B. Z. Reis, and S. M. F. Cozzolino, Brazil nuts: Nutritional composition, health benefits and safety aspects, Food Research International, **100** (2017) 9-18. https://doi.org/10.1016/j.foodres.2017.08.036.
5. H. P. Cornelio-Santiago, R. B. Bodini, and A. L. Oliveira, Potential of Oilseeds Native to Amazon and Brazilian Cerrado Biomes: Benefits, Chemical and Functional Properties, and Extraction Methods, *J. Am. Oil Chem. Soc.* **98** (2021) 3-20. https://doi.org/10.1002/aocs.12452.
6. A. Ibiapina, L. S. Gualberto, B. B. Dias, B. C. B. Freitas, G. A. S. Martins, and A. A. M. Filho, Essential and fixed oils from Amazonian fruits: properties and applications, *Critical Reviews in Food Science and Nutrition*, **62** (2021) 8842, https://doi.org/10.1080/10408398.2021.1935702.
7. F. D. Gunstone, Vegetable Oils in Food Technology: Composition, Properties and Uses, (John Wiley Sons, 2011). https://doi.org/10.1002/9781444339925.
8. J. M. deMan in: CK Chow (Ed) Fatty Acids in Foods and their Health Implications, Cap. 2, (2007), pp. 17-45.
9. R. D. O'brien, Fats and Oils: Formulating and Processing for Applications, (CRC press, Boca Raton, 2008). https://doi.org/10.1201/9781420061673
10. R. Zhang *et al.*, Enhancing Nutraceutical Bioavailability from Raw and Cooked Vegetables Using Excipient Emulsions: Influence of Lipid Type on Carotenoid Bioaccessibility from Carrots, *J. Agric. Food Chem.* **63** (2015) 10508, https://doi.org/10.1021/acs.jafc.5b04691
11. M. L. S. Albuquerque *et al.* Characterization of Buriti (Mauritia flexuosa L.) oil by absorption and emission spectroscopies, *J. Braz. Chem. Soc.* **16** (2005) 1113, https://doi.org/10.1590/S0103-50532005000700004
12. E. Choe, and D. B. Min, Chemistry of deep-fat frying oils, *J. Food Sci.* **72** (2007) 77-86. https://doi.org/10.1111/j.1750-3841.2007.00352.x
13. A. Thomas, B. Matthäus, and H. Fiebig, Fats and fatty oils, (Wiley Online Library, 2015), pp. 1-84. https://doi.org/10.1002/14356007.a10_173.pub2
14. A. L. S. Carvalho, M. C. Martelli, S. C. C. Nascimento, and D. S. B. Brasil, Brazil Nut oil: extraction methods and industrial applications Research, *Society and Development*, **11** (2022) e29511427256, https://doi.org/10.33448/rsd-v11i4.27256
15. M. Meenu, E. A. Decker, and B. Xu, Application of vibrational spectroscopic techniques for determination of thermal degradation of frying oils and fats: a review, *Critical Reviews in Food Science and Nutrition*, **21** (2021) 5744, https://doi.org/10.1080/10408398.2021.1891520
16. H. Lam, P. K. Roy, S. Chattopadhyay, Thermal degradation in edible oils by surface enhanced Raman spectroscopy calibrated with iodine values, *Vib. Spectrosc.*, **106** (2020) 103018, https://doi.org/10.1016/j.vibspec.2019.103018.
17. C. Lee, W. Yang, and R. G. Parr, Development of the Colle-Salvetti correlation-energy formula into a functional of the electron density, *Phys. Rev. B* **98** (1988) 785, https://doi.org/10.1103/PhysRevB.37.785.
18. X. Wu, S. Gao, J. S. Wang, H. Wang, Y. W. Huanga, Y. Zhaod, The surface-enhanced Raman spectra of aflatoxins: spectral analysis, density functional theory calculation, detection and differentiation, *Anlst.*, **137** (2012) 4226, https://doi.org/10.1039/C2AN35378D.
19. E. R. Davidson, Comment on Comment on Dunning's correlation-consistent basis sets, *Chem. Phys. Lett.*, **260** (1996) 514, https://doi.org/10.1016/0009-2614(96)00917-7
20. M.H. Jamróz, Vibrational Energy Distribution Analysis (VEDA): Scopes and limitations, *Spectrochim. Acta A Mol. Biomol. Spectrosc.*, **114** (2013) 220, https://doi.org/10.1016/j.saa.2013.05.096.

21. M.J. Frisch *et al.*, *Gaussian* **09** (Wallingford, CT, USA: Gaussian, 2009).

22. A. D. Becke, Density-functional thermochemistry III. The role of exact exchange, *J. Chem. Phys.* **98** (1993) 5648, https://doi.org/10.1063/1.464913.

23. T. Yanai, D. Tew, and N. Handy, A new hybrid exchange-correlation functional using the Coulomb-attenuating method (CAM-B3LYP), *Chem. Phys. Lett.*, **393** (2004) 51, https://doi.org/10.1016/j.cplett.2004.06.011

24. W. S. Martini, B. L. S. Porto, M. A. L. Oliveira, and A. C. Santana, Comparative Study of the Lipid Profiles of Oils from Kernels of Peanut, Babassu, Coconut, Castor and Grape by GC-FID and Raman Spectroscopy, *J. Braz. Chem. Soc.* **29** (2018) 390, https://dx.doi.org/10.21577/0103-5053.20170152.

25. J. R. Beattie, S. E. J. Bell, B. W. Moss, A critical evaluation of Raman spectroscopy for the analysis of lipids: Fatty acid methyl esters, *Lipids*, **39** (2004) 407. https://doi.org/10.1007/s11745-004-1245-z

26. S. Mahesar, S. T. H. Sherazi, A. R. Khaskheli, A. A. Kandhro, and S. Uddin, Analytical approaches for the assessment of free fatty acids in oils and fats, *Anal. Methods*, **6** (2014) 4956, https://doi.org/10.1039/C4AY00344F

27. J. Qiu, H. Hou, I. Yang, and X. Chen, Raman Spectroscopy Analysis of Free Fatty Acid in Olive Oil, *Appl. Sci.* **9** (2019) 4510. https://doi.org/10.3390/app9214510

28. V. Baeten, Raman spectroscopy in lipid analysis, *Lipid Technol.* **22** (2010) 36, https://doi.org/10.1002/lite.200900082.

29. H. Schulz, M. Baranska, Identification and quantification of valuable plant substances by IR and Raman spectroscopy, *Vib. Spectrosc.* **43** (2007) 13, https://doi.org/10.1016/j.vibspec.2006.06.001

30. F. Huang *et al.*, Identification of waste cooking oil and vegetable oil via Raman spectroscopy, *J. Raman Spectrosc.* **47** (2016) 860, https://doi.org/10.1002/jrs.4895.

31. S.K. Ku *et al.*, The harmful effects of consumption of repeatedly heated edible oils: a short review. *Clin Ter.* **4** (2014) 217, https://pubmed.ncbi.nlm.nih.gov/25203337/

32. Q. Zhang, A.S.M. Saleh, J. Chen, snd Q. Shen, Chemical alterations taken place during deep-fat frying based on certain reaction products: A review, *Chemistry and Physics of Lipids*, **6** (2012) 662, https://doi.org/10.1016/j.chemphyslip.2012.07.002

33. R. M. El-Abassy, P. Donfack, and A. Materny, Visible Raman spectroscopy for the discrimination of olive oils from different vegetable oils and the detection of adulteration, *J. Raman Spectrosc.* **40** (2009) 1284-1289. https://doi.org/10.1002/jrs.2279

34. M. Bennion and F. Hanning, Effect of different fats and oils and their modification on changes during frying, *Food Technology*, **10** (1956) 229-232.

35. S.H. Yoon, S.K. Kim, K.H. Kim, T.W. Kwon, and Y.K. Teah, Evaluation of physicochemical changes in cooking oil during heating, *J. Am. Oil Chem. Soc.*, **64** (1987) 870, https://doi.org/10.1007/BF02641496

36. G. Yen, C. Shao, C. Chen, and P. Duh, Effects of Antioxidant and Cholesterol on Smoke Point of Oils, *LWT - Food Science and Technology*, **30** (1997) 648, https://doi.org/10.1006/fstl.1996.0236

37. J.E. Albuquerque, B.C.L. Santiago, J.C.C. Campos, A.M. Reis, C.L. Silva, J.P. Martins, J.S.R. Coimbra, Photoacoustic Spectroscopy as an Approach to Assess Chemical Modifications in Edible Oils, *Journal of the Brazilian Chemical Society*, **3** (2013), https://doi.org/10.5935/0103-5053.20130047

38. I. P. R. Falco, N. G. Teruel, S. P. Moya, M. L. M. Carratalá, Kinetic study of olive oil degradation monitored by Fourier transform infrared spectrometry. Application to oil characterization, *J Agric Food Chem.* **47** (2012) 11800, https://doi.org/10.1021/jf3035918

39. M. Poiana, G.A. Mousdis, C.A. Georgiou, E. Alexa, D. Moigradean, I. Cocan, Detection of thermal processing impact on olive and sunflower oil quality by FTIR spectroscopy, *Journal of Agroalimentary Processes and Technologies*, **19** (2013) 48, https://journal-of-agroalimentary.ro/cauta?termen=detection

40. Y. Li, T. Fang, S. Zhu, F. Huang, Z. Chen, dmg Y. Wang, Detection of olive oil adulteration with waste cooking oil via Raman spectroscopy combined with iPLS and SiPLS, *Spectrochim. Acta A*, **189** (2018) 37, https://doi.org/10.1016/j.saa.2017.06.049

41. L. Hocevar, V. R. B. Soares, F. S. Oliveira, M. G. A. Korn, L. S. G. Teixeira, Application of multivariate analysis in mid-infrared spectroscopy as a tool for the evaluation of waste frying oil blends, *J. Am. Oil. Chem. Soc.* **89** (2011) 781, https://doi.org/10.1007/s11746-011-1968-8.

42. M. Y. Talpur *et al.*, A simplified FTIR chemometric method for simultaneous determination of four oxidation parameters of frying canola oil, *Spectrochim. Acta A*, **149** (2015) 656, https://doi.org/10.1016/j.saa.2015.04.098

43. A. M. Marina, Y. B. Che Man, S. A. H. Nazimah, I. Amin, Chemical Properties of Virgin Coconut Oil, *J. Am. Oil Chem. Soc.* **86** (2009) 301, https://doi.org/10.1007/s11746-009-1351-1.

44. Q. S. Martins, P. V. Almeida, Q. S. Ferreira, A. Oliveira, C. Aguirre, and J. L. B. Faria, Investigation of ostrich oil via Raman and infrared spectroscopy and predictions using the DFT method, *Vibrational Spectroscopy*, **104** (2019) 102945, https://doi.org/10.1016/j.vibspec.2019.102945

45. M. P. Andersson, P. Uvdal, New Scale Factors for Harmonic Vibrational Frequencies Using the B3LYP Density Functional Method with the Triple-ζ Basis Set 6-311+G(d,p), *The Journal of Physical Chemistry A*, **109** (2005) 2937, https://doi.org/10.1021/jp045733a.

46. D. Russell, Johnson III (Ed.), Computational Chemistry Comparison and Benchmark Database, NIST Standard Reference Database, Release 22, NIST, 2022. https://doi.org/10.18434/T47C7Z

47. J. McMurry, Organic chemistry; 9 Ed.; (Cengage Learning, Boston, MA, USA, 2016).

48. M. Çınar, B. Alim, Z. Alim, E. Şakar, Determination of the molecular structure and spectroscopic properties of capsaicin, *Radiation Physics and Chemistry*, **208** (2023) 110879, http://dx.doi.org/10.2139/ssrn.4292963

49. J. A. Antunes *et al.*, Study on optical, electrochemical and thermal properties of the Meldrum acid 5-aminomethylene derivative, *Vib. Spectrosc.* **112** (2021) 103188, https://doi.org/10.1016/j.vibspec.2020.103188.